Flow, Turbulence and Combustion **63:** 443–477, 1999.

Reynolds Number Dependence of Energy Spectra in the Overlap Region of Isotropic Turbulence

STEPHAN GAMARD and WILLIAM K. GEORGE
Department of Mechanical and Aerospace Engineering, State University of New York, Buffalo, NY 14260, U.S.A.

Abstract. A Near-Asymptotics analysis of the turbulence energy spectrum is presented that accounts for the effects of finite Reynolds number recently reported by Mydlarski and Warhaft [21]. From dimensional and physical considerations (following Kolmogorov and von Karman), proper scalings are defined for both low and high wavenumbers, but with functions describing the entire range of the spectrum. The scaling for low wavenumbers uses the kinetic energy and the integral scale, L, based on the integral of the correlation function. The fact that the two scaled profiles describe the *entire* spectrum for *finite* values of Reynolds number, but reduce to different profiles in the limit, is used to determine their functional forms in the "overlap" region that both retain in the limit. The spectra in the overlap follow a power law, $E(k) = Ck^{-5/3+\mu}$, where μ and C are Reynolds number dependent. In the limit of infinite Reynolds number, $\mu \to 0$ and $C \to$ constant, so the Kolmogorov/Obukhov theory is recovered in the limit. Explicit expressions for μ and the other parameters are obtained, and these are compared to the Mydlarski/Warhaft data. To get a better estimate of the exponent from the experimental data, existing models for low and high wavenumbers are modified to account for the Reynolds number dependence. They are then used to build a spectral model covering all the range of wavenumbers at every Reynolds number. Experimental data from grid-generated turbulence are examined and found to be in good agreement with the theory and the model. Finally, from the theory and data, an explicit form for the Reynolds number dependence of $\phi = \varepsilon L/u^3$ is obtained.

Key words: energy spectrum, isotropic, overlap region, near asymptotics, energy decay, Reynolds number effect.

1. Introduction

In 1941 Kolmogorov [15] introduced his ideas for the similarity of small scale turbulence and the inertial subrange. This was subsequently extended to the energy spectrum by Obukhov [22] who first derived the famous $k^{-5/3}$-law. In spite of the modifications by Kolmogorov himself [16], and apart from recent questions about universality, for more than fifty years this theory has been widely discussed and more or less accepted. An often overlooked assumption in Kolmogorov's theory, however, is the necessity of "*a sufficiently large Reynolds number*" before the assumptions can be expected to hold. This qualification is especially relevant since there are few spectral measurements which unequivocally show a $k^{-5/3}$ spectral

range. And even those were made at very high Reynolds numbers, well above those for which the theory is commonly applied.

In 1996, Mydlarski and Warhaft [21] proposed, on experimental grounds, that the exponent in the inertial subrange in fact was not the $-5/3$ proposed by Kolmogorov, but rather a function of the Reynolds number that perhaps went to $-5/3$ in the limit of infinite Reynolds number. For all the Reynolds numbers of their experiments, the spectrum rolled-off *more slowly* than $k^{-5/3}$; moreover, the lower the Reynolds number the greater the difference.

As noted above, there have been numerous theoretical attempts to modify the exponent in the power law, first suggested by Kolmogorov [16] himself, mostly to account for internal intermittency (see [4] for a review). But these deviations from the $k^{-5/3}$ behavior can not explain the Mydlarski and Warhaft observations, since all arguments for internal intermittency cause the spectrum to roll-off *faster* than $k^{-5/3}$, *not slower*.

Recently George [6, 8] (see also [9]) proposed two ideas which allow treatment of finite Reynolds number effects in turbulent flows when infinite Reynolds number forms of the equations are available. The first is the Asymptotic Invariance Principle (AIP) which states that properly scaled solutions at infinite Reynolds number must be similarity solutions to the limiting equations themselves. Thus the determination of scaling parameters is determined by the equations themselves, not by *ad hoc* arguments. The second is the methodology of Near-Asymptotics which provides a means to find overlap solutions at finite Reynolds number when inner and outer forms of the limiting equations are available. These ideas were successfully applied to a number of wall-bounded turbulent flows.

This paper theoretically justifies Mydlarski and Warhaft's conclusions by applying the AIP and Near-Asymptotics to the spectral energy equation for isotropic turbulence. The results will be seen to be in remarkable agreement with the data, thereby providing additional confirmation *from the governing equations* for both the experiments and the methodology. An interesting (and perhaps even surprising) outcome of this work will be an analytical expression for the Reynolds number dependence of the important ratio $L/l = \varepsilon L/u^3$ where L is the physical integral scale.

2. Theoretical Analysis

2.1. Basic equations and definitions

Following Batchelor [2], we will use the energy spectrum function, $E(k,t)$, defined by integrating the energy tensor Φ_{ii} over spherical shells of values k, i.e.,

$$E(k,t) = \frac{1}{2} \iint\limits_{k=|\underline{k}|} \Phi_{ii}(\underline{k})\, \mathrm{d}\sigma(\underline{k}), \tag{1}$$

where $d\sigma(\underline{k})$ is an element of surface in wavenumber space at radius $k = \underline{k}$, and Φ_{ii} is the trace of the Fourier transform of the two-point velocity correlation tensor given by

$$\Phi_{ij}(\underline{k}) = \frac{1}{8\pi^3} \iiint_{-\infty}^{\infty} e^{-i\underline{k}\cdot\underline{r}} \overline{u_i(\underline{x})\, u_j(\underline{x}+\underline{r})}\, d\underline{r}. \tag{2}$$

Note that $E(k, t)$ is a scalar function of only the magnitude $k = |\underline{k}|$, hence the directional information has been removed. Also, hereafter the time-dependence of E will be suppressed and it will be written simply as $E(k)$.

The integral of E over all wavenumbers k yields the turbulence energy:

$$\frac{3}{2}u^2 = \frac{1}{2}\overline{u_i u_i} = \int_0^{\infty} E(k)\, dk. \tag{3}$$

The rate of dissipation of turbulent kinetic energy per unit mass (or simply the dissipation rate), ε, is related to the energy spectrum by

$$\varepsilon = 2\nu \int_0^{\infty} k^2\, E(k)\, dk. \tag{4}$$

For isotropic turbulent flow the energy equation reduces to a balance among simply the time rate of change of the energy spectrum, $\partial E/\partial t$, the energy transfer between different wavenumbers, T, and the viscous dissipation, $2\nu k^2 E$, i.e.,

$$\frac{\partial E(k)}{\partial t} = T(k) - 2\nu\, k^2\, E(k). \tag{5}$$

The energy spectrum typically rises from zero at $k = 0$ to a peak value at a wavenumber near the inverse of the integral scale defined below, then rolls-off for higher wavenumbers. Hence the energy is dominated by wavenumbers around the peak. Viscous stresses dominate the highest wavenumbers and make the primary contribution to the dissipation integral.

2.2. THE LENGTH SCALES

2.2.1. *The Integral Length Scale*

There exists much confusion about which scales are really appropriate to the description of the energy spectrum at large scales. We shall refer to the large scale we consider most important as the *physical integral scale, L*, and define it from the integral of the longitudinal velocity correlation:

– Longitudinal integral scale:

$$L \equiv \frac{1}{\overline{u_1^2}} \int_0^\infty \overline{u_1(x, y, z, t) u_1(x + r, y, z, t)}\, \mathrm{d}r. \tag{6}$$

– For isotropic turbulence, L can equivalently be obtained from the energy spectrum function as:

$$L = \frac{3\pi}{4} \frac{\int_0^\infty E(k)/k\, \mathrm{d}k}{\int_0^\infty E(k)\, \mathrm{d}k}. \tag{7}$$

Thus, L is completely determined once $E(k)$ is given.

It is important to note that the "physical" integral scale differs from the "*pseudo*" integral scale ($l \simeq u^3/\varepsilon$) often found in the literature (and used by Mydlarski and Warhaft as well). It will be argued below that the ratio $L/l = \phi$ is *Reynolds number dependent* and constant only in the limit of infinite Reynolds number; i.e.,

$$\frac{L}{l} = \frac{\varepsilon L}{u^3} \equiv \phi(R). \tag{8}$$

2.2.2. *The Kolmogorov Microscale*

The other important length scale of importance to the analysis presented below is the Kolmogorov microscale, η. Using Kolmogorov's second hypothesis which implies that the only parameters in the equilibrium range *in the infinite Reynolds number limit* are ε and the viscosity ν, it follows that the length scale is given by:

$$\eta = \left(\frac{\nu^3}{\varepsilon}\right)^{1/4}. \tag{9}$$

This scale is characteristic of the high wavenumber part of the spectrum since it is of the order of the smallest eddies found in homogeneous turbulence.

2.2.3. *The Reynolds Number*

We define a Reynolds number, R, based on the ratio of the length scales given by:

$$R = \frac{L}{\eta}. \tag{10}$$

Note that this differs from the definition of Reynolds number of $R_l = ul/\nu$ used in many texts (cf. [26]). Here $R_l = (R/\phi(R))^{4/3}$.

2.3. SIMILARITY CONSIDERATIONS

2.3.1. *Similarity Scalings for Low and High Wavenumbers*

A dimensional analysis of the energy spectrum shows its proportionality to the product of a length and the square of a characteristic velocity. Following Batchelor, it has been customary to scale the spectrum in two ways:

– Low wavenumber (or energy variables) using u and L (or l); say

$$\bar{k} = kL,$$
$$f_L(\bar{k}, R) = \frac{E(k,t)}{u^2 L}. \tag{11}$$

– High wavenumber (or Kolmogorov variables) using η, $u_\eta \equiv (\nu\varepsilon)^{1/4}$; say

$$k^+ = k\eta,$$
$$f_H(k^+, R) = \frac{E(k,t)}{u_\eta^2 \eta} = \frac{E(k,t)}{\varepsilon^{1/4}\nu^{5/4}}. \tag{12}$$

The first form of Equation (11) was originally suggested by von Karman and Howarth [27], while the latter was first proposed by Obukhov [22].

Note that it is commonly assumed that the Kolmogorov scale *collapses* the spectral data at high wavenumbers, regardless of the Reynolds number. This cannot be exactly the case, however, since the whole idea of an equilibrium range in the spectrum at high wavenumbers is predicated on the separation of scales [2]. The Kolmogorov scaling can at most represent an infinite Reynolds number limit to which finite Reynolds number spectra asymptote as the turbulent Reynolds number increases. Thus, regardless of which set of parameters the spectrum is scaled by, either retain a Reynolds number dependence for finite values of R. It is this weak (and asymptotically vanishing) dependence on Reynolds number which is explored in the analysis below, and which will be seen to be responsible for the observations of Mydlarski and Warhaft [21].

It is important to note that both f_L and f_H represent exactly the same spectrum since, at least at finite Reynolds number, they are just different non-dimensionalizations of the same function. Because of this it follows immediately that:

$$f_L(\bar{k}, R) = R^{-5/3}\,\phi^{2/3}\, f_H(k^+, R). \tag{13}$$

In the limit of infinite Reynolds number however, f_H becomes independent of R and loses the ability to describe the low wavenumber spectral behavior. Similarly

f_L becomes independent of R but loses the ability to describe the dissipation range. But both retain an inertial subrange in the limit, a $k^{-5/3}$ range which extends to infinity for the low wavenumber scaled forms and to zero for the high. This has long been recognized and is represented in most texts (cf. [26]).

This can be argued in a slightly different way. In the limit of infinite Reynolds number f_L and f_H are similarity solutions of different limiting forms of Equation (5). (This is straightforward to show by substituting the low and high wavenumber scaled versions of Equations (11) and (12) in Equation (5), and carrying out the limit as $R \to \infty$.) For finite values of k, the low wavenumber form reduces in the limit to a simple balance between the temporal decay and the spectral transfer *to* the high wavenumbers, say ε_k. The high wavenumber form reduces to the familiar local equilibrium range [2], where there is simply a balance between the dissipation and the spectral transfer *from* the low wavenumbers, but this is just ε_k. Since all of the energy dissipated in this limit must come via the spectral flux from low wavenumbers, then $\varepsilon_k = \varepsilon$ (but only in the limit). Thus for the low wavenumbers in the limit of infinite Reynolds number, the only parameters are the energy, u^2 and the dissipation, ε. And for the high wavenumbers the only parameters are the dissipation, ε, and the kinematic viscosity, ν. Hence u^2 and ε *alone* govern the low wavenumber spectrum *exactly* in the limit, while ν and ε *alone* govern *exactly* the high. Thus in the limit of infinite Reynolds number, both the von Karman/Howarth and Kolmogorov scalings become exact and independent of Reynolds number, i.e.,

$$\lim_{R\to\infty} f_L(\overline{k}, R) = f_{L\infty}(\overline{k}) \text{ only,}$$

and

$$\lim_{R\to\infty} f_H(k^+, R) = f_{H\infty}(k^+) \text{ only.}$$

This is, of course, the whole idea behind scaling in the first place; namely that the spectra should collapse, at least in the limit. And in this case they do since they are similarity solutions to equations which themselves become independent of the Reynolds number in the limit as $R = L/\eta \to \infty$. This is, in fact, the Asymptotic Invariance Principle of George [8].

Obviously $f_{L\infty}(\overline{k})$ and $f_{H\infty}(k^+)$ can not have the same functional dependence on k, except possibly in an overlap region (the so-called *inertial subrange*). In fact, as is well known, at low wavenumbers, $f_{H\infty} \to k^{+-5/3}$ while for high wavenumbers $f_{L\infty} \to \overline{k}^{-5/3}$ [26]. It will be seen to be possible below using the methodology of Near-Asymptotics to extend this reasoning to finite Reynolds numbers, and deduce the Mydlarski and Warhaft results from first principles without additional assumptions.

2.4. MATCHING OF THE TWO PROFILES

The low and high wavenumber spectra have been scaled with different scales. But *the ratio of those scales is Reynolds number dependent.* Therefore, *at finite Reynolds numbers, there cannot exist any region in which either scaling is truly Reynolds number independent*. Note that this does not mean the scaled spectra will not collapse approximately, only that perfect collapse can be achieved only in the limit. It is this lack of perfect collapse at finite Reynolds numbers which is the key to understanding the analysis below.

Now as long as we consider only finite Reynolds numbers, $f_L(\overline{k}, R)$ and $f_H(k^+, R)$ represent the spectrum for all wavenumbers. It is only in the limit as $R \to \infty$ that f_L loses the ability to describe the high wavenumbers and f_H the low. The traditional asymptotic matching begins with the limiting forms, $f_{L\infty}$ and $f_{H\infty}$, and tries to stretch their region of validity to match them in an overlap region (if such a region exists). Such an analysis for the energy spectra is presented in [26], and the resulting "matched region" is the $k^{-5/3}$-region, or inertial subrange.

If, however, we consider the *finite* Reynolds number forms instead of the limiting ones, the problem of solving the overlap region can be approached in a different way. Since both f_L and f_H already describe the entire spectrum, there is no need to stretch their range of validity and match them. They already match perfectly at all wavenumbers, but have simply been scaled differently. Instead, our problem is that these finite Reynolds number functions degenerate in different ways at infinite Reynolds number, one losing high wavenumbers, the other the low. Our objective is to use this information to determine their functional form *in the remaining common region they describe in this limit* (if it exists). This methodology is known as *Near-Asymptotics* and was first developed in [8] (see also [9, 10]). In the following paragraphs it is applied to the energy spectrum.

Even if we do not know the analytical forms of f_L and f_H, we can still use their properties. Both describe the same spectrum, so they must satisfy

$$u^2 \, L \, f_L(\overline{k}, R) = (\varepsilon \, \nu^5)^{1/4} \, f_H(k^+, R). \tag{14}$$

Equivalently, using the definition of $R = L/\eta$ and defining

$$\phi = \frac{\varepsilon \, L}{u^3}, \tag{15}$$

we can write

$$f_L(\overline{k}, R) = R^{-5/3} \, \phi^{2/3} \, f_H(k^+, R). \tag{16}$$

The function $\phi(R)$ is the ratio of the physical integral scale, L, to the pseudo-integral scale, $l = u^3/\varepsilon$. The Kolmogorov reasoning summarized above implies that $\phi \to$ constant in the limit as $R \to \infty$. As noted earlier, it is only in this limit that L and l can be used interchangeably.

To simplify the following expressions, we define g as

$$g(R) = R^{-5/3} \, \phi^{2/3}. \tag{17}$$

Now we can re-write Equation (16) simply as

$$f_L(\overline{k}, R) = g(R) f_H(k^+, R). \tag{18}$$

As for the spectra themselves, the partial derivatives with respect to k and R for both high and low wavenumbers forms of the spectrum must be the same for finite values of R. Differentiating with respect to k while holding R constant implies:

$$\frac{\partial}{\partial k}\left((u^2\, L) f_L(\overline{k}, R)\right)\bigg|_R = \frac{\partial}{\partial k}\left((\varepsilon\, \nu^5)^{1/4} f_H(k^+, R)\right)\bigg|_R. \tag{19}$$

Or in dimensionless form,

$$\frac{\overline{k}}{f_L}\,\frac{\partial f_L}{\partial \overline{k}}\bigg|_R = \frac{k^+}{f_H}\,\frac{\partial f_H}{\partial k^+}\bigg|_R. \tag{20}$$

We want to examine if there is an overlap region that survives in both f_L and f_H when $R \to \infty$ and

$$\begin{cases} \overline{k} & \to \infty, \\ k^+ & \to 0. \end{cases}$$

Since $\overline{k}/k^+ = R$, in order to remain in the overlap region in the limit, should it exist, we need to define an intermediate variable, k_n:

$$\begin{aligned} k_n &= \overline{k} \cdot R^{-n} \\ &= k^+ \cdot R^{1-n}. \end{aligned} \tag{21}$$

We can fix our position in the overlap region, and simultaneously satisfy $\overline{k} \to \infty$ and $k^+ \to 0$ as $R \to \infty$ if we choose $0 < n < 1$.

Introducing k_n in Equation (18):

$$f_L(\overbrace{k_n\, R^n}^{\overline{k}}, R) = g(R)\, f_H(\overbrace{k_n\, R^{n-1}}^{k^+}, R). \tag{22}$$

We can now differentiate with respect to R *at fixed* k_n to obtain

$$\frac{\partial f_L}{\partial \overline{k}}\bigg|_R \frac{\partial \overline{k}}{\partial R}\bigg|_{k_n} + \frac{\partial f_L}{\partial R}\bigg|_{\overline{k}} = \frac{\mathrm{d}g}{\mathrm{d}R} f_H + g\left[\frac{\partial f_H}{\partial k^+}\bigg|_R \frac{\partial k^+}{\partial R}\bigg|_{k_n} + \frac{\partial f_H}{\partial R}\bigg|_{k^+}\right]. \tag{23}$$

Using Equation (21) and multiplying by $R/f_L = R/(g\, f_H)$:

$$\begin{aligned} & n\,\frac{\overline{k}}{f_L}\,\frac{\partial f_L}{\partial \overline{k}}\bigg|_R - (n-1)\,\frac{k^+}{f_H}\,\frac{\partial f_H}{\partial k^+}\bigg|_R \\ & \quad = \frac{R}{g}\frac{\mathrm{d}g}{\mathrm{d}R} + R\left[\frac{1}{f_H}\frac{\partial f_H}{\partial R}\bigg|_{k^+} - \frac{1}{f_L}\frac{\partial f_L}{\partial R}\bigg|_{\overline{k}}\right]. \end{aligned} \tag{24}$$

Since the first term on the right-hand side is a function of R only, we define $\gamma(R)$ by

$$\gamma(R) \equiv \frac{R}{g}\frac{\mathrm{d}g}{\mathrm{d}R} = \frac{\mathrm{d}(\ln g)}{\mathrm{d}\ln R}, \tag{25}$$

and S_L and S_H by

$$S_L(\overline{k}, R) \equiv \left.\frac{\partial \ln f_L(\overline{k}, R)}{\partial \ln R}\right|_{\overline{k}}, \tag{26}$$

$$S_H(k^+, R) \equiv \left.\frac{\partial \ln f_H(k^+, R)}{\partial \ln R}\right|_{k^+}. \tag{27}$$

Now Equation (24) can be written as

$$\left.\frac{\overline{k}}{f_L}\frac{\partial f_L}{\partial \overline{k}}\right|_R = \left.\frac{k^+}{f_H}\frac{\partial f_H}{\partial k^+}\right|_R = \gamma(R) + [S_H(k^+, R) - S_L(\overline{k}, R)]. \tag{28}$$

As noted earlier, in the limit as $R \to \infty$, both f_L and f_H become asymptotically independent of R, each losing in the process the ability to describe part of the spectrum. Thus, from the definitions of S_L and S_H, the term in square brackets in Equation (28) must vanish identically. This leaves only the first term which must go to a constant, i.e.,

$$\lim_{R\to\infty}\left.\frac{\overline{k}}{f_L}\frac{\partial f_L}{\partial \overline{k}}\right|_R = \lim_{R\to\infty}\left.\frac{k^+}{f_H}\frac{\partial f_H}{\partial k^+}\right|_R = \lim_{R\to\infty}\gamma(R) \equiv \gamma_\infty. \tag{29}$$

So there is indeed a common part which survives in this limit. We shall see below that the constant, $\gamma_\infty = -5/3$, so the Kolmorogov/Obukhov result is obtained as the infinite R limit.

The question of most interest, however, is: what happens at large but finite Reynolds numbers? In other words, is there any wavenumber region where

$$\left.\frac{\overline{k}}{f_L}\frac{\partial f_L}{\partial \overline{k}}\right|_R = \left.\frac{k^+}{f_H}\frac{\partial f_H}{\partial k^+}\right|_R \approx \gamma(R), \tag{30}$$

even when $|\gamma(R) - \gamma_\infty| > 0$? If so, we have found the explanation for the Mydlarski and Warhaft results.

To examine this, we look how S_L and S_H are changing with $\ln R$. A Taylor expansion about a given value of R at fixed k yields:

$$S_L(\overline{k}, R) \simeq \frac{f_L(\overline{k}, R + \Delta R) - f_L(\overline{k}, R)}{f_L(\overline{k}, R)}\frac{R}{\Delta R}, \tag{31}$$

and

$$S_H(k^+, R) \simeq \frac{f_H(k^+, R + \Delta R) - f_H(k^+, R)}{f_H(k^+, R)} \frac{R}{\Delta R}. \tag{32}$$

Thus S_L and S_H represent the relative Reynolds number dependencies of f_L and f_H. They must, of course, vanish in the limit of infinite Reynolds number since the scaled spectra are similarity solutions to the limiting equations. At finite Reynolds numbers, S_L goes from near zero for small values of $\overline{k}$ where the low wavenumber scaling is approximately correct, and increases as $\overline{k}$ becomes large since the low wavenumber scaling does apply at the dissipative scales. For S_H, it is just the opposite, large for small k^+ and decreasing toward zero as k^+ approaches infinity. The whole question of whether there is an overlap region at finite Reynolds number then reduces to whether there is a common region where $|S_H - S_L| \ll \gamma(R)$. Another possibility would be that $S_L = S_H$, namely that both scaling profiles have the same R dependence. We shall assume there is such a region, and show this leads to a consistent approximation.

Therefore, we neglect $(S_H - S_L)$ relative to $\gamma(R)$ and write simply

$$\left.\frac{\overline{k}}{f_L}\frac{\partial f_L}{\partial \overline{k}}\right|_R = \gamma(R), \tag{33}$$

$$\left.\frac{k^+}{f_H}\frac{\partial f_H}{\partial k^+}\right|_R = \gamma(R). \tag{34}$$

The solutions to these equations must be recognized as first-order approximations only, the higher order contributions having been neglected. They do, however, reduce to the correct limiting solutions, and retain at least that Reynolds number dependent part of the solution which is independent of wavenumber. The neglect of $S_H - S_L$ must be and can be justified *a posteriori*.

Integrating Equations (33) and (34) leads immediately to *Reynolds number dependent* power laws for both f_L and f_H, i.e.,

$$f_L(\overline{k}, R) = C_L(R)\,(\overline{k})^{\gamma(R)}, \tag{35}$$

$$f_H(k^+, R) = C_H(R)\,(k^+)^{\gamma(R)}. \tag{36}$$

Substituting the definition of g (Equation (17)) into Equation (25) yields

$$\gamma = -5/3 + \mu, \tag{37}$$

where μ has been defined to be

$$\mu = \frac{2}{3}\frac{\mathrm{d}\ln\phi}{\mathrm{d}\ln R}. \tag{38}$$

Note since $\phi \to$ constant as $R \to \infty$, this implies that $\mu \to 0$ in the same limit. But this in turn implies that $\gamma_\infty = -5/3$, which yields immediately the result obtained by Obukhov [22], as noted above.

By using Equation (18), we can express g as:

$$g(R) = \frac{f_L}{f_H} = \frac{C_L(R)}{C_H(R)} R^{-5/3+\mu(R)}. \tag{39}$$

Substituting $\gamma(R) = -5/3 + \mu$ from Equation (25) into Equation (39) shows that a solution is possible only if

$$\ln R \frac{\mathrm{d}\gamma}{\mathrm{d}\ln R} = \frac{\mathrm{d}\ln C_H/C_L}{\mathrm{d}\ln R}. \tag{40}$$

This equation makes it clear that μ, C_H and C_L are inter-related, and cannot simply be chosen arbitrarily. Also, it is easy to show that satisfying this constraint insures that $S_H - S_L \equiv 0$ for the overlap solution, consistent with the original hypothesis.

Like μ, C_H/C_L can also be shown to be simply related to $\phi(R)$. Comparing Equations (17) and (39), it follows immediately that

$$\frac{C_H}{C_L} = \phi^{-2/3} R^{\mu(R)}. \tag{41}$$

We know from the Kolmogorov argument presented above that $\phi \to \phi_\infty$ where ϕ_∞ is an non-zero constant. Also C_H and C_L must be finite and different from zero in the limit of infinite Reynolds number; otherwise the *scaled* spectra would either go to zero or increase without bound. But this is not physically possible, since they must represent exact similarity solutions of the governing equations in the limit of infinite Reynolds number. (In other words, the scaling itself would have to be wrong.) Taking the logarithm of Equation (41) yields

$$\ln \frac{C_H}{C_L} = -\frac{2}{3} \ln \phi + \mu \ln R. \tag{42}$$

It follows immediately that both C_H/C_L and ϕ can be non-zero constants in the limit as $R \to \infty$ only if $\mu \to 0$ *faster* than $1/\ln R$!⋆

Thus, everything about the Reynolds number dependence is contained in the unknown function, $\phi(R)$. If ϕ can be determined, all our functions will be known. Alternatively, if C_H/C_L is determined, then so is ϕ. Even the determination of μ allows ϕ to be expressed to within an integration constant. This latter possibility is the approach followed below.

It may seem surprising that the Reynolds number dependence of the overlap region is intimately linked to the Reynolds number dependence of $\phi = \varepsilon L/u^3$. As noted above, however, the asymptotic constancy of ϕ depends crucially on the Kolmogorov argument relating the spectral flux in the inertial subrange to the exact dissipation. Therefore it should not be surprising that these break down together at finite Reynolds number. Nor should it be surprising that a theory which accounts for the Reynolds number dependence of one, also accounts for the other.

All of the conditions can be satisfied in two ways:

⋆ This immediately rules out the "conjecture" of Barenblatt and Chorin [1] who take $\mu \sim 1/\ln R$.

– **Possibility 1 (Reynolds number *independent* overlap range)**:
$\phi \to$ constant, and $\mu = 0$ and the overlap region is Reynolds number independent.

Or ϕ must satisfy two conditions as $\ln R \to \infty$; namely:

– **Possibility 2 (Reynolds number *dependent* overlap range)**:

- *Condition* 1. $\phi \to \phi_\infty =$ constant.
- *Condition* 2. $\mu = (2/3)d\ln\phi/d\ln R \to 0$ faster than $1/\ln R$.

The first possibility leads to a $-5/3$ power-law which is independent of Reynolds number. Mydlarski and Warhaft [21] have shown, however, that the exponent of real data is Reynolds number dependent. Therefore it is the Reynolds number dependent solution of Possibility 2 that is of primary interest here.

3. The Function μ

The function μ can be completely determined only with a closure model for the turbulence. In the absence of that, we must resort to empirical forms. Even so, we know a great deal about its behavior. First, it is clear from Equation (40) that μ will be most naturally expressed in terms of the argument $\ln R$. Second, Condition 1 above can be satisfied only if μ depends on inverse powers of $\ln R$. In fact, if we expand about the infinite Reynolds number limit, μ must be asymptotically of the form:

$$\mu(\ln R) = \frac{\beta A}{(\ln R)^{1+\beta}}\left[1 + \frac{a_1}{\ln R} + \cdots\right], \tag{43}$$

where the constant βA is chosen of this form for convenience later. Note that Condition 2 can be satisfied only if $\beta > 0$. The consequences of failing to satisfy either condition are that similarity cannot be maintained in the overlap region. Clearly this would be unphysical since both the low and high wavenumber scalings are similarity solution to the energy equation in the limit.

George and Castillo [9] and George et al. [10] were successful by truncating Equation (43) at the first term. We shall do the same here, i.e.,

$$\mu = \frac{\beta A}{(\ln R)^{1+\beta}}, \tag{44}$$

where the only adjustable parameters are A and β. It follows immediately from Equation (38) that

$$\ln\frac{\phi}{\phi_\infty} = -\frac{3A}{2(\ln R)^\beta}. \tag{45}$$

Similarly, substitution into Equation (41) implies

$$\frac{C_H}{C_L} = \frac{C_{H\infty}}{C_{L\infty}} \exp\left[\frac{(1+\beta)A}{(\ln R)^\beta}\right]. \tag{46}$$

Thus all of the Reynolds number dependence of all the coefficients has been determined. Verification that Equations (44) to (46) are consistent with the spectral data *and* determination of the constants is the primary purpose of the data analysis described below.

4. The Experimental Data

4.1. One-dimensional versus three-dimensional spectra

To test and develop further the ideas above we used the raw spectral values (longitudinal and lateral one-dimensional half-line spectra⋆) obtained by Mydlarski and Warhaft [21] in a careful series of experiments. These were performed downstream of a variety of passive and active grids. The turbulence was effectively homogeneous across the flow and decayed slowly downstream.

For experimental reasons, a Fourier analysis with respect to one-space coordinate only is sometimes considered. The resulting spectrum function is a one-dimensional Fourier transform of the velocity correlation tensor:

$$\begin{aligned} F_{ij}^1(k_1) &= \frac{1}{2\pi}\int_{-\infty}^{\infty} \overline{u_i u_j}(r_1, 0, 0)\, \mathrm{e}^{-ik_1 r_1}\, \mathrm{d}r_1 \\ &= \iint_{-\infty}^{\infty} \Phi_{ij}(k_1, k_2, k_3)\, \mathrm{d}k_2\, \mathrm{d}k_3. \end{aligned} \tag{47}$$

The superscript 1 in F_{ij}^1 is there to emphasize the fact that the dependence in the k_2 and k_3-directions vanishes by integration, leaving only one in the k_1-direction. In the case $i = j = 1$, $F_{ij}^1(k_1)$ is called the *longitudinal* one-dimensional spectrum, while $i = j = 2$ is the *lateral* one-dimensional spectrum.

For isotropic turbulence, all of the one-dimensional spectra, F_{ij}^1 are simply related to the three-dimensional energy spectrum function (or simply the energy spectrum), $E(k)$. The two of interest here are

$$F_{11}^1(k_1) = \frac{1}{2}\int_{k_1}^{\infty} \frac{E(k)}{k}\left[1 - \left(\frac{k_1}{k}\right)^2\right] \mathrm{d}k, \tag{48}$$

$$F_{22}^1(k_1) = \frac{1}{4}\int_{k_1}^{\infty} \frac{E(k)}{k}\left[1 + \left(\frac{k_1}{k}\right)^2\right] \mathrm{d}k. \tag{49}$$

⋆ The half-line spectrum is simply double whole-line spectrum.

Also

$$E(k) = k^3 \frac{\mathrm{d}}{\mathrm{d}k}\left(\frac{1}{k}\frac{\mathrm{d}F_{11}^1}{\mathrm{d}k}\right). \tag{50}$$

It easy to show that, if there is a power law region where $E(k) = Ck^{-5/3+\mu}$, then there is a corresponding region in the one-dimensional spectra for which

$$F_{11}^1 = C_1 k_1^{-5/3+\mu}, \tag{51}$$

$$F_{22}^1 = C_2 k_1^{-5/3+\mu}, \tag{52}$$

where

$$C_1 = \frac{C}{(\frac{5}{3}-\mu)(\frac{11}{3}-\mu)}, \tag{53}$$

$$C_2 = \frac{(\frac{4}{3}-\mu)C}{(\frac{5}{3}-\mu)(\frac{11}{3}-\mu)} \tag{54}$$

and

$$\frac{F_{22}^1}{F_{11}^1} = \frac{4}{3} - \frac{\mu}{2}. \tag{55}$$

These reduce to the classical relations as $\mu \to 0$ (cf. [2]).

When considering actual data we shall need also the integral scales defined from the longitudinal and lateral velocity correlations or corresponding one-dimensional spectra, $F_{ij}^1(k_1)$, which were what Mydlarski and Warhaft actually measured. These definitions are:

– Longitudinal integral scale:

$$\begin{aligned} L_1 &= \frac{1}{\overline{u_1^2}} \int_0^\infty \overline{u_1(x, y, z, t)u_1(x + r, y, z, t)}\,\mathrm{d}r \\ &= \frac{\pi}{\overline{u_1^2}} \lim_{k_1 \to 0} F_{11}^1(k_1). \end{aligned} \tag{56}$$

– Lateral one-dimensional spectrum:

$$\begin{aligned} L_2 &= \frac{1}{\overline{u_2^2}} \int_0^\infty \overline{u_2(x, y, z, t)u_2(x + r, y, z, t)}\,\mathrm{d}r \\ &= \frac{\pi}{\overline{u_2^2}} \lim_{k_1 \to 0} F_{22}^1(k_1). \end{aligned} \tag{57}$$

For isotropic turbulence $L = L_1 = 2L_2$, a condition not exactly satisfied by the data, but easily dealt with as we shall show later. The values of ε were determined by integrating the one-dimensional spectral data and using $\varepsilon = \varepsilon_1 + 2\varepsilon_2$ where ε_α is defined by:

$$\varepsilon_\alpha = 5 \int_0^\infty k_1^2 F_{\alpha\alpha}^1(k_1)\, \mathrm{d}k_1. \tag{58}$$

4.2. THE HIGH WAVENUMBER SCALING

The one-dimensional spectral data in high wavenumber variables is shown in Figure 1.

This is the classical Kolmogorov scaling (Equation (12)), and has been shown to be reasonably successful at high wavenumbers in many experiments. Such is the case here. As expected, the scaled spectra clearly separate at low wavenumbers where the scaling in no longer appropriate. This behavior with Reynolds number of the spectrum at low wavenumbers is also expected (cf. [26]), and is a direct consequence of the arguments presented previously. Note that, contrary to expectations, there is not a consistent trend with Reynolds numbers at low wavenumbers. This perhaps can be attributed to the difference between the initial conditions for the various grids.

4.3. THE LOW WAVENUMBER SCALING

The low wavenumber scaling (Equation (11)) needs the integral scale for the one-dimensional half-line spectrum. Only the pseudo-integral scale was used by Mydlarski and Warhaft who took $l = 0.9u^3/\varepsilon$. Therefore, a determination of L_1 and L_2 was essential. The spectra can not be determined at zero wavenumbers, of course, because of record length limitations. Moreover, the spectral errors cannot be removed by the usual smoothing since there are fewer estimates at these low wavenumbers. The one-dimensional spectra at the origin ($k_1 = 0$) can be expanded, however, as

$$F_{11}^1 = A_1 - B_1 k_1^2 + C_1 k_1^4, \tag{59}$$

$$F_{22}^1 = A_2 + \frac{1}{2} B_2 k_1^2, \tag{60}$$

where $B_1 = B_2$ if the turbulence is isotropic [26]. By fitting the curves to the measured spectra at the lowest wavenumbers, it was possible to extrapolate to "zero wavenumber" values without being dependent on simply the lowest wavenumber data alone. The values of the different integral scales are presented in Table I.

The integral scales do not satisfy the isotropic relations. Therefore, we plotted the longitudinal spectra using $F_{11}^1/\overline{u_1^2}\, L_1$ *versus* $k_1 L_1$; and the lateral spectra as

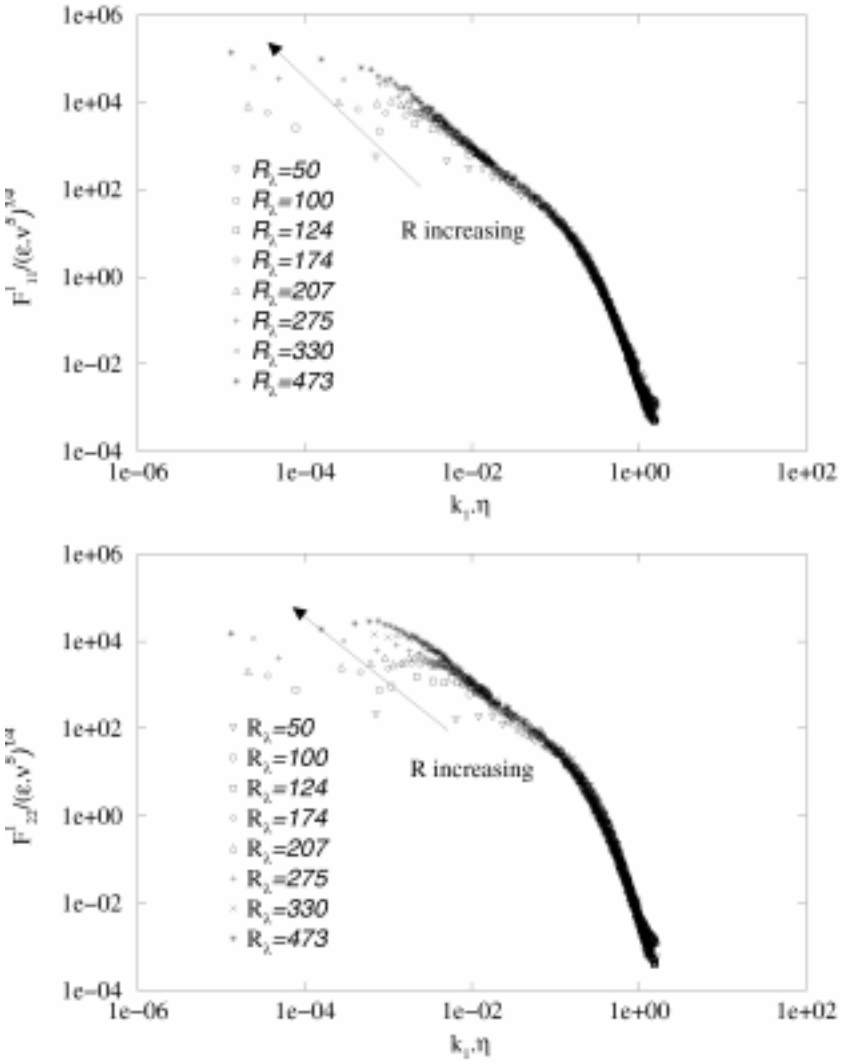

Figure 1. One-dimensional spectra in high wavenumber scaling.

Table I. The integral scales (in meter).

R_λ	50	100	124	174	207	275	330	473
L_1	0.0226	0.0648	0.0483	0.0532	0.0500	0.1364	0.1054	0.1218
L_2	0.0076	0.0213	0.0196	0.0180	0.0198	0.0346	0.0356	0.0398
u^3/ε	0.0158	0.0533	0.0581	0.0662	0.0703	0.1253	0.1257	0.1648

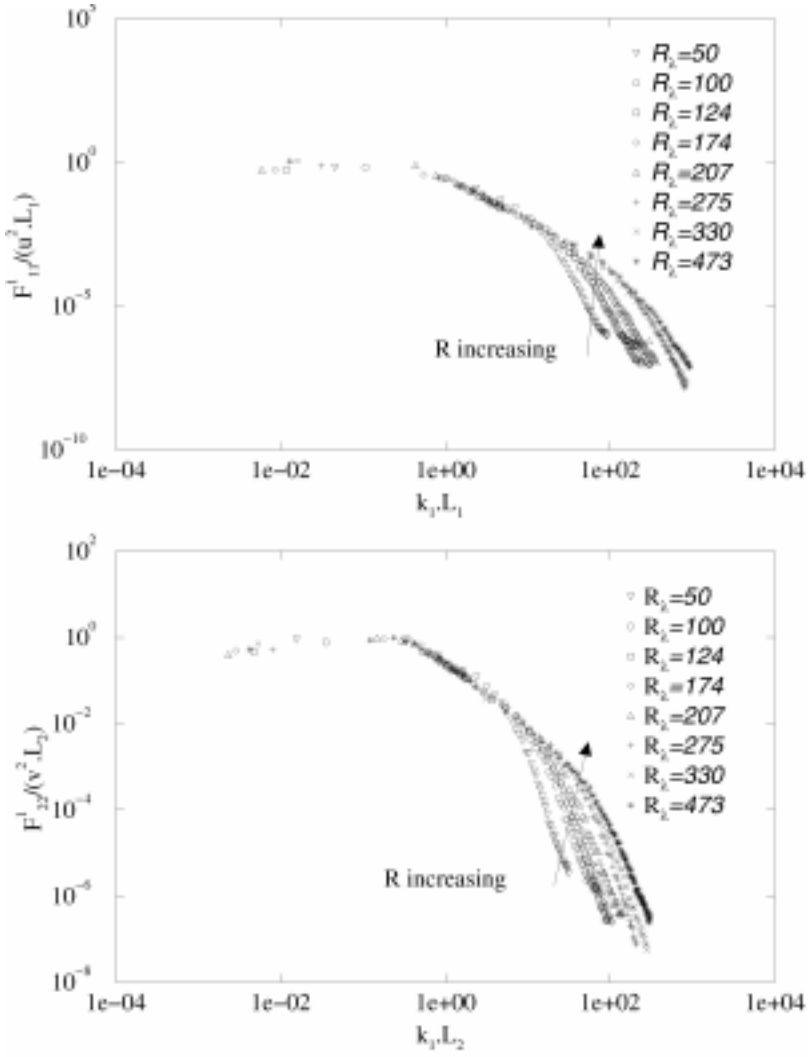

Figure 2. One-dimensional spectra in low wavenumber scaling.

$F_{22}^1/\overline{u_2^2}\,L_2$ *versus* $k_1 L_2$. As shown in Figure 2, both show a good collapse except for the high wavenumbers where the scaling is no longer appropriate. The lack of a consistent Reynolds numbers' trend at high wavenumbers outside the collapse zone is also present here, just as for the high wavenumber scaling.

Figure 3 shows the same spectra non-dimensionalized with u and $l = 0.9u^3/\varepsilon$, the pseudo-integral scale used by Mydlarski and Warhaft. Although the differences are slight, the physical integral scale L_1 (or L_2) is the better choice. Note that either L or l could have been used in the analysis above, but the results obtained using L are more useful since the Reynolds number dependence of the ratio L/l appears explicitly in μ instead of in $S_H - S_L$.

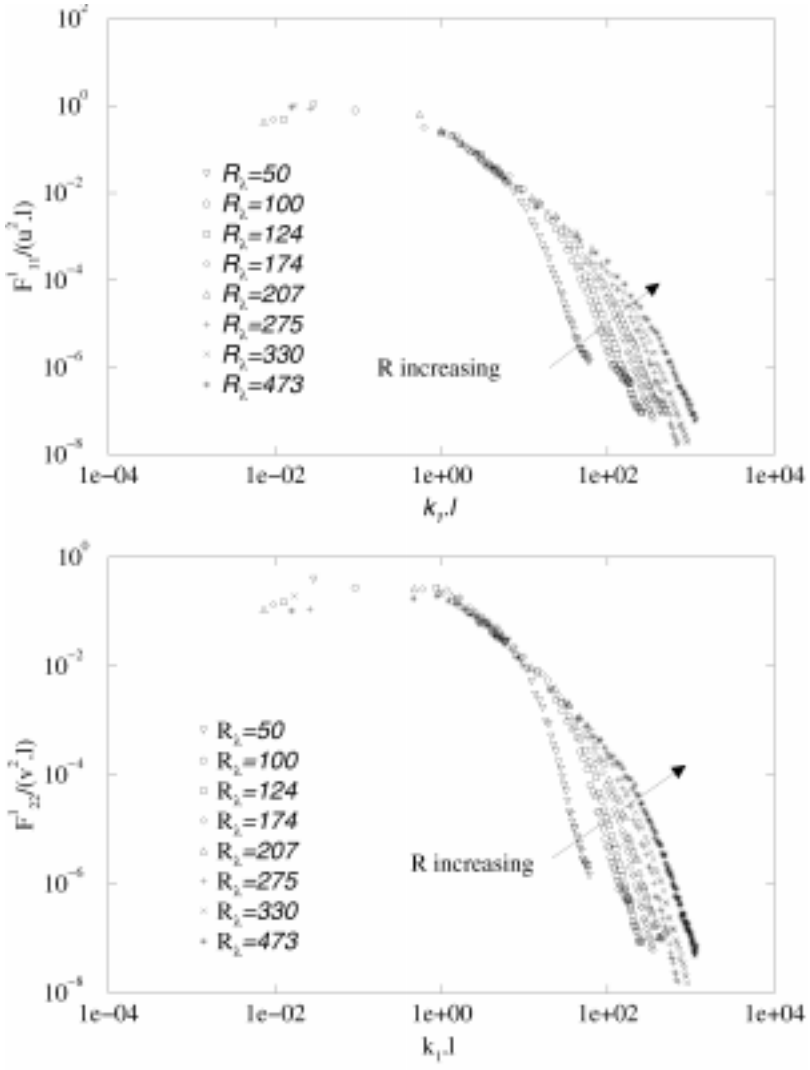

Figure 3. One-dimensional spectra scaled with u and l, the pseudo-integral scale.

4.4. DETERMINATION OF μ, C_H AND C_L FROM THE DATA

Figure 4 illustrates the Mydlarski and Warhaft conclusions quite simply. When the spectrum is multiplied by $k^{+5/3}$, none of the spectra show the flat region implied by a $-5/3$ power law. This is consistent with our theory, both that the power is not $-5/3$ for any of the data, and that this value can at most be approached asymptotically. Nonetheless, there is always some subjectivity in the determination of μ. Mydlarski and Warhaft [21] chose the best exponent, n, to enable $k_1^n.F^1_{\alpha\alpha}$ to achieve a constant plateau. (Note that $n = -5/3 + \mu$.) They did not, however, utilize the isotropic properties of their spectra; and thus, cited two different values

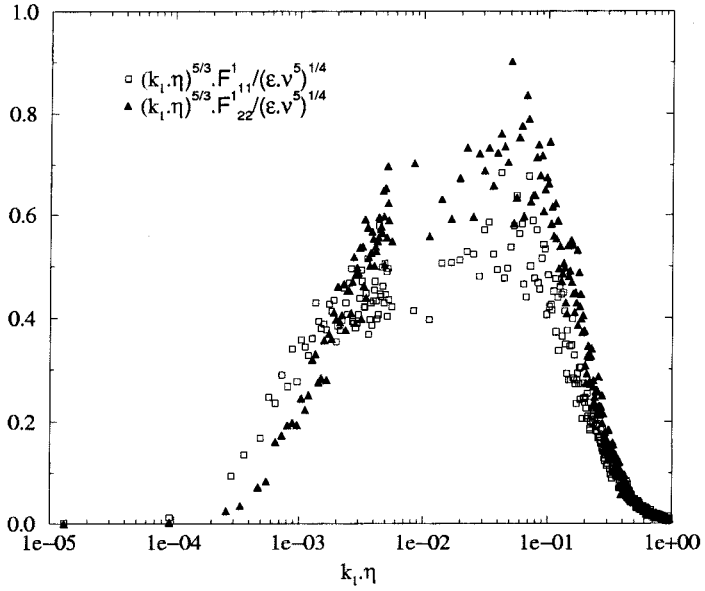

Figure 4. One-dimensional spectra in high wavenumber scaling multiplied by $k^{+5/3}_1$.

for μ: one for the longitudinal part of the spectrum and one for the lateral part. In our analysis of the same data, we treated the longitudinal and lateral spectra together using the isotropic conditions above. This, in effect, doubles the amount of data that can be used and reduces the statistical error. Two different methods were applied to the data to obtain independent estimates of the parameters μ, C_H, and C_L (and from them A and β in Equation (44)):

Method 1 begins with plots in inner and outer variables of

$$\frac{k_1}{F^1_{11}}\frac{\mathrm{d}F^1_{11}}{\mathrm{d}k_1}, \tag{61}$$

and

$$\frac{k_1}{F^1_{22}}\frac{\mathrm{d}F^1_{22}}{\mathrm{d}k_1}, \tag{62}$$

where the derivatives were computed directly from the data. It is easy to show that in the power law region (if there is one) these are equal to $-5/3 + \mu$. A typical result is illustrated in Figure 5. Once μ is found in this manner, the values of $C_{H\alpha}$ and $C_{L\alpha}$ are read on the curves of $F^{+1}_{\alpha\alpha}\,(k^+_1)^{5/3-\mu}$ and $\overline{F}^1_{\alpha\alpha}\,(\overline{k}_1)^{5/3-\mu}$, similar to the approach of Mydlarski and Warhaft.

Method 2 was developed to deal with the fact that both of the above methods have difficulty distinguishing unambiguously precisely what data should be included in

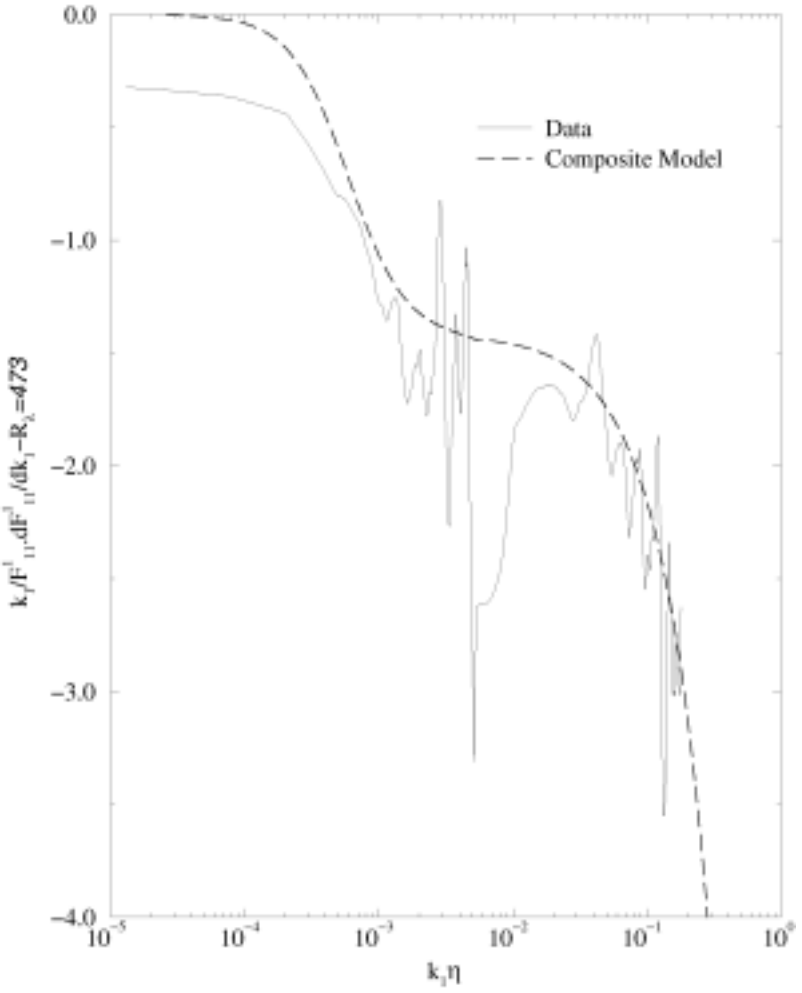

Figure 5. Derivation of μ using $(k^+/f_H)(\partial f_H/\partial k^+) = -5/3 + \mu(R)$ for $R_\lambda = 473$.

the overlap region. This is because both the low and high wavenumber regions have some residual influence on it, especially at the lowest Reynolds numbers. This is a common problem in applying any asymptotic theory to real data, and is illustrated by Figure 6 which plots the result of applying Method 2 to the high and low wavenumber semi-empirical spectral models discussed in the Appendix.

Also plotted is the composite spectrum obtained by multiplying them together and dividing by the common part. (These spectral models are discussed in detail in the Appendix to avoid interrupting the main theme of this paper.) While the high wavenumber model asymptotes to $k^{-5/3+\mu}$ at low wavenumbers, and the low to the same at high wavenumbers, their product never achieves this value – exactly like the real data!

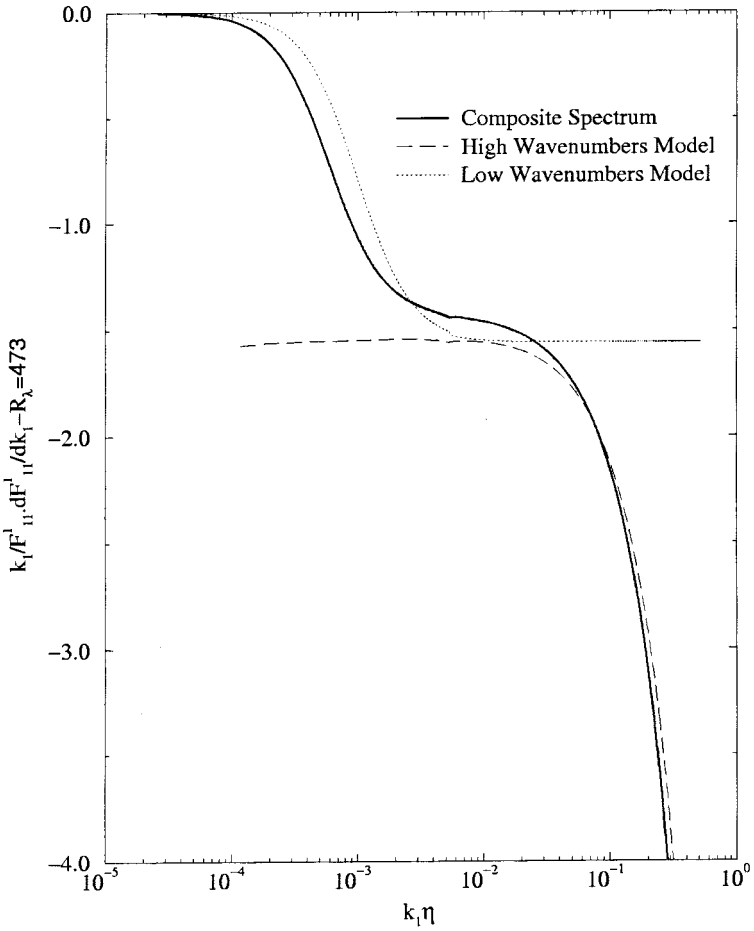

Figure 6. Derivation of μ using $(k^+/f_H)(\partial f_H/\partial k^+) = -5/3 + \mu(R)$ for $R_\lambda = 473$ using semi-empirical spectra models.

To avoid this problem we have used the composite spectral model to fit the entire spectrum for every Reynolds number. This was done using an optimization routine, first to find the optimum values of μ, C_H and C_L for each spectrum separately, then to optimize the constants in Equations (44) and (46) above. The fits of the composite model to all the Mydlarski/Warhaft spectra (high wavenumber variables) are shown in Figures 7 and 8.

Over the entire range of Reynolds numbers, the agreement between model and experimental is spectacular, as are the same spectra in low wavenumber variables.

The values of μ are summarized in Table II, together with the original Mydlarski and Warhaft values.

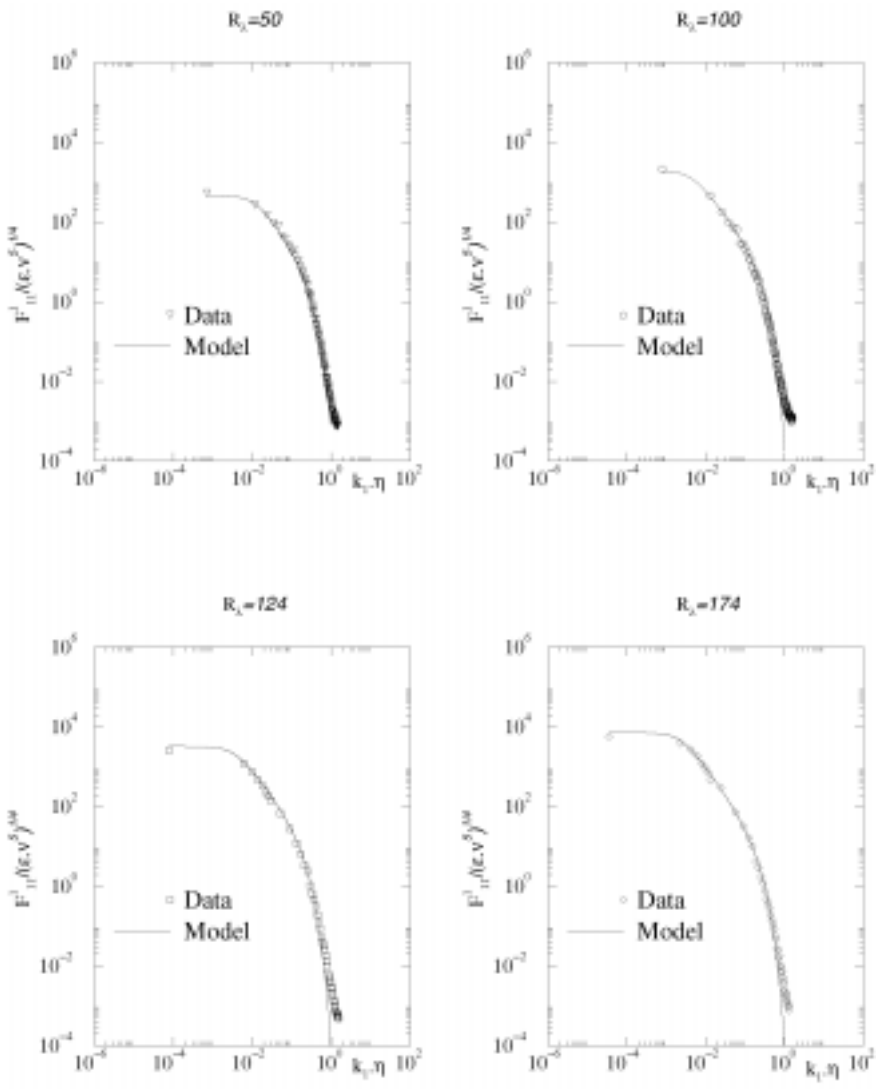

Figure 7. The composite model for the first four Reynolds numbers.

5. Evaluation of the Spectral Theory

Equations (44) and (46) were applied to the values found for μ, C_H, and C_L. Then, those values were used as starting points to optimize the spectral fit to the original data. We found the optimal choice of constants to be

$$A = 4.22, \quad \beta = 0.87, \tag{63}$$

so that μ is given by:

$$\mu(R) = \frac{3.69}{(\ln R)^{1.87}}. \tag{64}$$

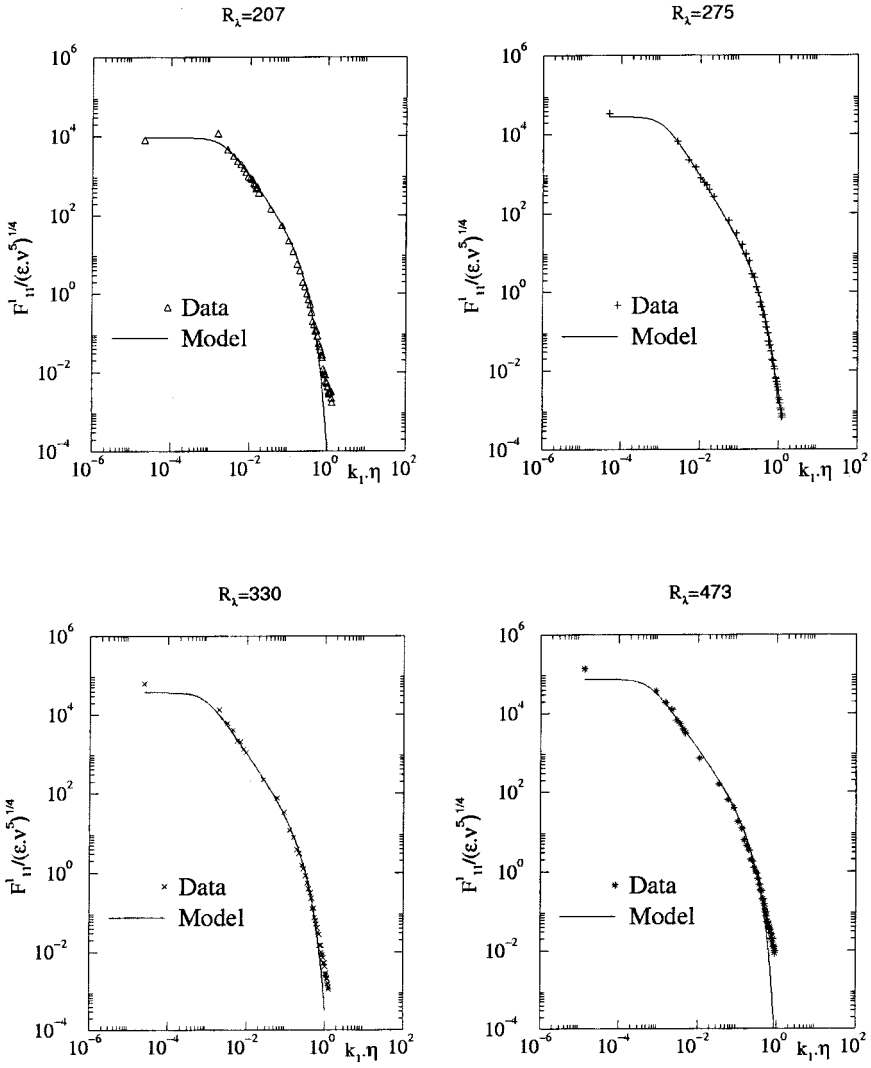

Figure 8. The composite model for the last four Reynolds numbers.

The corresponding result for C_H/C_L is:

$$\frac{C_H}{C_L} = \frac{C_{H\infty}}{C_{L\infty}} \exp\left[\frac{7.91}{(\ln R)^{0.87}}\right] \tag{65}$$

with $C_{H\infty}/C_{L\infty} = 0.59$. (Note that $C_{H\infty} \neq C_{L\infty}$ as in the analysis of Tennekes and Lumley [26] because the infinite Reynolds number limit of L/l is not exactly unity.)

The values for μ and C_H/C_L from the spectral fit are quite close to the ones found with the data analysis alone (cf. Table II). The only major discrepancies

Table II. Summary on the values of μ.

R_λ	Present work			Warhaft and Mydlarski	
	Data analysis	Composite spectrum	$A\beta/\ln R^{1+\beta}$	μ_1	μ_2
50	0.43	0.13	0.25	0.37	0.57
100	0.19	0.19	0.19	0.37	0.37
124	0.18	0.18	0.18	0.17	0.27
174	0.14	0.14	0.15	0.15	0.21
207	0.13	0.13	0.14	0.15	0.21
275	0.11	0.02	0.11	0.13	0.21
330	0.11	0.09	0.11	0.11	0.15
473	0.11	0.11	0.10	0.09	0.11

Table III. Implementation of the model $\mu = 3.69/(\ln R^{1.87})$.

R_λ	50	100	124	174	207	275	330	473
μ	0.25	0.19	0.18	0.15	0.14	0.11	0.11	0.10
C_H/C_L	5.75	4.21	4.08	3.54	3.40	2.78	2.77	2.55

were for $R_\lambda = 50$ and $R_\lambda = 275$. It is our opinion that there is no real overlap region for the $R_\lambda = 50$ data. Moreover, the problem with the $R_\lambda = 275$ spectra can probably be attributed to the lack of isotropy.

The values for the particular Reynolds numbers of interest have been included in Table III.

We summarize results for μ in Figure 9, and for C_H/C_L in Figure 10. These figures also include the earlier values found by Mydlarski and Warhaft [21] for the longitudinal one-dimensional spectrum. We have also added Barenblatt and Chorin's hypothesis [1] to emphasize its non-fit, which is not too surprising since it contradicts both the Kolmogorov and von Karman/Howarth scalings simultaneously in the limit as $L/\eta \to \infty$.

Figure 10 shows C_H/C_L as a function of R for the two one-dimensional spectra. The scatter in the values is due to the fact that the coefficient C_L (or C_H) is highly dependent on the value of μ: a small change in μ can give an important difference in the value of C. Clearly the theory and the proposed model are both consistent with the experimental data; moreover they have the correct asymptotic limits.

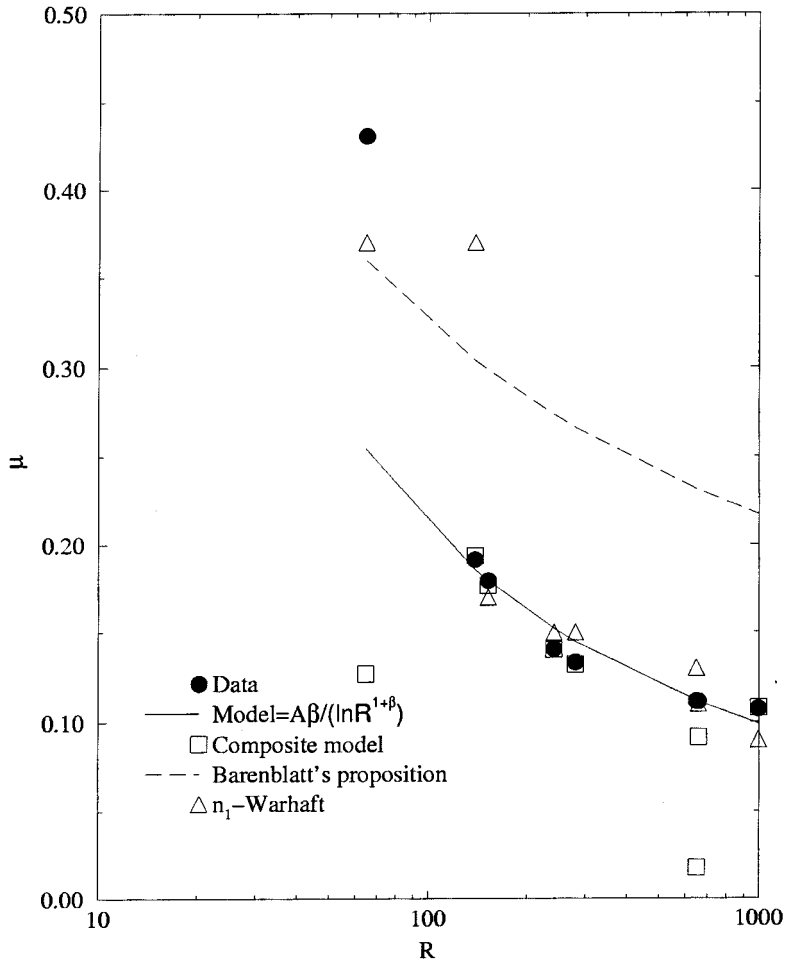

Figure 9. Different values of μ function of the Reynolds number.

6. The Function $\phi(R)$

A somewhat surprising benefit of the spectral analysis was a determination of the Reynolds number dependence of the length scale ratio $L/l = \phi(R)$. This has relevance, not only to the present analysis, but to many types of turbulence models (cf. [17, 18]).

From Equations (45) and (63) it follows immediately that:

$$\frac{\phi}{\phi_\infty} = \exp\left\{-\frac{6.34}{(\ln R)^{0.87}}\right\}. \tag{66}$$

The value ϕ_∞ can immediately be obtained from Equation (41) as

$$\phi_\infty = \left\{\frac{C_{H\infty}}{C_{L\infty}}\right\}^{-3/2} = 2.20. \tag{67}$$

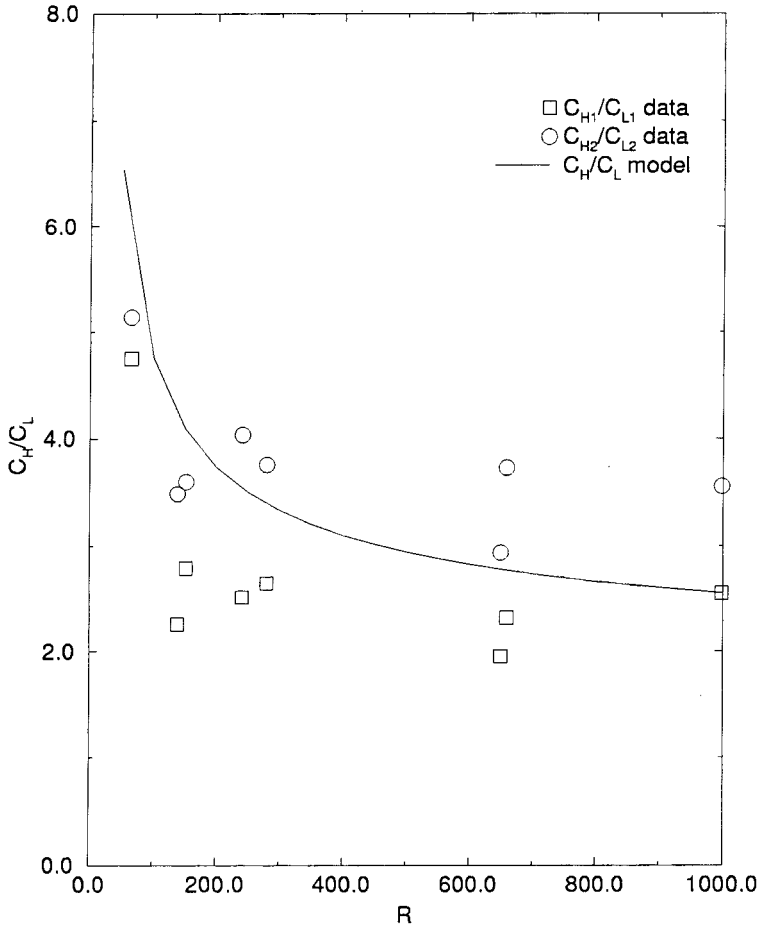

Figure 10. Different values of C_H/C_L function of the Reynolds number.

This result is shown in Figure 11, along with the values of L_1/l and $2L_2/l$ obtained earlier. Note that for isotropy $2L_2 = L_1$ (hence the factor 2). As noted earlier, however, the integral scales did not satisfy the isotropic relations. Therefore we have also plotted $[L_1+2(2L_2)]/3l$ which is an attempt to produce a better estimate for comparison by averaging the longitudinal integral scale with the other two, assuming the latter to be equal.

The theoretical curve *with constants determined only from the spectra* does reasonably well at high values of R, but goes in the wrong direction for low values. It will be argued below that the low Reynolds number behavior of the data is because of the nature of the dissipation at low wavenumbers. Therefore we have also plotted the limiting form for small values and a composite of both the high and low forms together. These are discussed in the next paragraph.

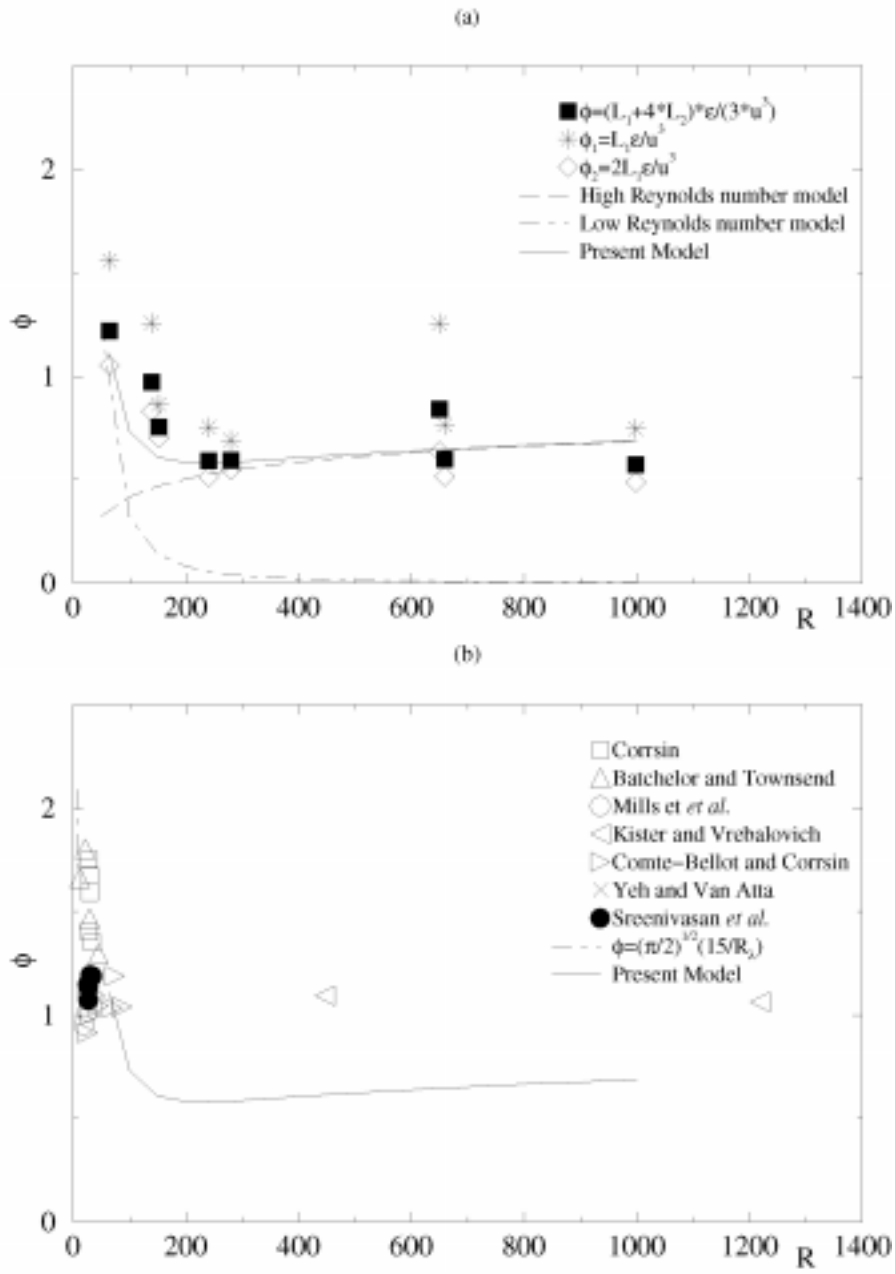

Figure 11. ϕ function of the Reynolds number. Part (a) shows Equations (70), (69), and (66) together with the Mydlarski/Warhaft data; (b) Equation (70) with data taken from Sreenivasan [25].

Table IV. Values of ϕ from data and model of Equation (70).

R_λ	50	100	124	174	207	275	330	473
Data	1.22	0.97	0.75	0.59	0.59	0.84	0.60	0.57
Model	1.11	0.62	0.60	0.58	0.58	0.64	0.64	0.68

It is well known (cf. [26]) that in the limit as $R \to 0$,

$$\lim_{R\to 0} \varepsilon = D\nu \frac{u^2}{L^2}. \tag{68}$$

It follows immediately that

$$\lim_{R\to 0} \phi = \frac{D^{3/2}}{R^2}. \tag{69}$$

A simple composite form, reminiscent of those commonly used in turbulence modeling (cf. [11]) can be created by combining the two expressions, i.e.,

$$\phi_{\text{comp}} = \frac{D^{3/2}}{R^2} + 2.20 \exp\left\{-\frac{6.34}{(\ln R)^{0.87}}\right\}. \tag{70}$$

This is the limiting form plotted in Figure 11a with $D = 215$. The values are found in Table IV. This does a reasonably good job of describing the experimental data (in spite of the lack of isotropy), except for the L_1 from the problematical $R_\lambda = 275$ *grid*. A most striking feature of the composite curve is that ϕ is nearly independent of R for $R > 200$. This apparent cancellation of competing effects explains the willingness of the turbulence community to assume $L/l \approx$ constant (cf. [2, 25]). Figure 11b shows the semi-empirical relation of Equation (70) plotted together with data from Sreenivasan [25]. The agreement at low wavenumbers is excellent; only the high Reynolds number asymptotes differ. It might be significant, however, that all of those data were taken from the controversial experiment of Kistler and Vrebalovich [14].

A major contributor to the scatter in all the plots might be the tendency of grid-generated turbulence to fall into the form of similarity decay described by George [7]. A consequence of this is that the energy decays so that $(\varepsilon L/u^3)R_\lambda =$ constant, but where the constant is determined by the upstream conditions. Therefore, the farther the measuring point downstream, the higher the value of ϕ (for fixed initial conditions). In general, the higher the Reynolds number of the grid, the higher the constant, but also the slower the variation of R_λ downstream. Thus, unless the grid geometry and measuring point relative to it were fixed (i.e., fixed x/M), this effect will act to produce artificially high values of ϕ, especially for small R. This is consistent with what is observed, but is impossible to quantify without further experimentation.

7. Conclusions

In the previous sections, we have developed a theory for the energy spectrum at finite Reynolds numbers. We considered two ranges of wavenumbers (classified as low and high), and have defined the appropriate length scales for each region: the physical integral scale, that we believe is the appropriate length scale for the low wavenumber region, and the Kolmogorov scale, η, for the high wavenumber region.

Based on the energy equation and on its evolution at infinite Reynolds numbers, we have derived the appropriate parameters for the two regions of interest. Those parameters are u and ε for the low wavenumber region (also being the region containing the energy), and ν and ε for the high wavenumber one (being the dissipation region). We can then scale the entire spectrum for the whole range of wavenumbers, at least at finite Reynolds number. Only in the limit of infinite Reynolds numbers do they lose the ability to describe the entire spectrum, one losing the low, the other the high range of wavenumbers.

For finite Reynolds numbers the two differently scaled energy spectra must still represent the same spectral function. We were able to use this fact with Near-Asymptotics to determine the conditions for and properties of an overlap region shared by the two similarity functions that survive in the limit of an infinite Reynolds number. We proved that the spectrum should follow a power law k^n in the overlap, where the exponent, $n = -5/3 + \mu$, is Reynolds number dependent but goes to $-5/3$ in the limit of infinite Reynolds number, thus recovering in the limit the Obukhov/Kolmogorov result.

To verify the above theory, we needed a set of isotropic decaying or grid turbulence data which covered a wide range of Reynolds numbers. Such a set already existed from the experiments of Mydlarski and Warhaft [21]. When their data was plotted in both low and high wavenumbers variables, we found a near perfect collapse in the expected regions, proving that the appropriate length scale for low wavenumbers is really the physical integral scale L, and that the exponent is indeed Reynolds number dependent.

The data for μ, however, contained some scatter, and left some doubts concerning its value. We therefore developed an empirical spectral model allowing a Reynolds number dependent exponent in the overlap region. To do so, we created a multiplicative composite spectrum based on a low wavenumber model (extended from a von Karman one) and on a high wavenumber one (extended from a Lin/Hill version). This composite model was then applied on the data sets for a better evaluation of μ. The results mostly confirmed our previous estimates (and those of Mydlarski and Warhaft as well). We then optimized the choice of $\mu = \beta A/(\ln R)^{1+\beta}$ (where A and β were the only free parameters) to fit this composite spectrum to all the spectral data.

The theory also predicted other functional relationships including the coefficients for the power law region and the behavior of $\phi = \varepsilon L/u^3$. All predictions

were well-confirmed by the theory. When the low Reynolds number asymptote was used to create a composite equation for ϕ covering all Reynolds numbers, it became clear why most experimentalists believe this ratio to be nearly constant for all but the lowest Reynolds numbers.

It remains to relate the conclusions of this Near-Asymptotic analysis to a full similarity analysis of decaying turbulence for fixed initial (or upstream) conditions. It is not clear, for example, when *local similarity theories* like that discussed here apply, and when *full similarity* takes over. It appears, however, that the former determines the value of the constants for the latter, but this will require further careful study. Of particular utility would be experiments which carefully distinguish between development downstream with fixed upstream conditions, and families of experiments where only the upstream Reynolds number was varied with all other features fixed.

Acknowledgements

We would like to express our gratitude to Professors L. Mydlarski (McGill University) and Z. Warhaft (Cornell University), both for sharing their data and for their encouragement during the course of this work. The bulk of this work and the details for most of it can be found in the MS Thesis of SG at SUNY/Buffalo. We would like to acknowledge the support of the National Science Foundation during part of this work.

Appendix: Empirical Spectral Models

It has been customary to consider two classes of spectral models: a low wavenumber one and a high wavenumber one. Traditionally, a low wavenumber model should roll off a $k^{-5/3}$ and never reach the dissipation range. An example is the von Karman model considered below. The high wavenumber model, by contrast, starts as $k^{-5/3}$ then rolls off exponentially with increasing wavenumbers.

Our goal in this Appendix is to modify two of these existing infinite Reynolds number models to incorporate the effect of finite Reynolds number. Then following Driscoll [3] or Helland et al. [12], we will then "marry" these two models to create a composite model to cover all the wavenumber range.

A LOW WAVENUMBER MODEL

At low wavenumbers, the energy spectrum starts from zero wavenumber as k^n where $1 < n < 4$ [7]. Von Karman and others have gotten reasonable agreement with grid generated turbulence by using $n = 4$ and the following functional form:

$$E(x) = B\frac{x^4}{(1+x^2)^{17/6}}, \tag{71}$$

where $x = k/k_e$, B and k_e must be determined. Note that the k^4 dependence at low wavenumbers has little effect on the one-dimensional spectrum, and other values could be used.

To incorporate the finite Reynolds number form in the matching region, we simply modify the above model:

$$E_{low}(x) = B\frac{x^4}{(1+x^2)^{17/6-\mu/2}}. \tag{72}$$

If we assume isotropy, we can relate E to F_{11}^1. Moreover, we can determine B and k_e if we use the relations between u^2 and the integral scale and F_{11}^1 (since, at low wavenumbers, u^2 and L_1 are the proper scaling parameters). It is straightforward to show that

$$k_e = \frac{\sqrt{\pi}\,\Gamma\left(\frac{5}{6}-\frac{\mu}{2}\right)}{L_1\,\Gamma\left(\frac{1}{3}-\frac{\mu}{2}\right)}, \tag{73}$$

where Γ is the Euler–Gamma function.

Therefore, the one-dimensional low wavenumber form of the one-dimensional longitudinal spectrum becomes

$$F_{11}^1(k_1) = \frac{u^2\,L_1}{\pi}\left(1+x_1^2\right)^{-5/6+\mu/2}. \tag{74}$$

This model is valid for low wavenumber scaling; hence, as $k_1 L_1 \to \infty$ (or $x_1 \to \infty$),

$$\begin{aligned} F_{11}^1 \;&\to\; \frac{u^2\,L_1}{\pi}\left(\frac{k_1\,L_1}{k_e\,L_1}\right)^{-5/3+\mu} \qquad \text{(model limit)},\\ &=\; u^2\,L_1\,C_{L1}\,(k_1\,L_1)^{-5/3+\mu} \qquad \text{(power form)}. \end{aligned}$$

Clearly these two equations require:

$$C_{L1} = \frac{1}{\pi}\,(k_e\,L_1)^{5/3-\mu}, \tag{75}$$

where both μ and C_{L1} depends on the Reynolds number. A fit to the set of data at $R_\lambda = 473$ can be seen in Figure 12 (upper).

A HIGH WAVENUMBER MODEL

There are numerous examples of high wavenumber spectral models. Monin and Yaglom [20], for instance have an extensive review. We will consider in this work an improvement of the Lin/Hill model, which seems to reproduce the spectral behavior the best. This model originated from Corrsin and Pao's [23, 24] ideas on modeling ε_k as a function of E and k, in addition to ε. Later on, Lin [19] improved

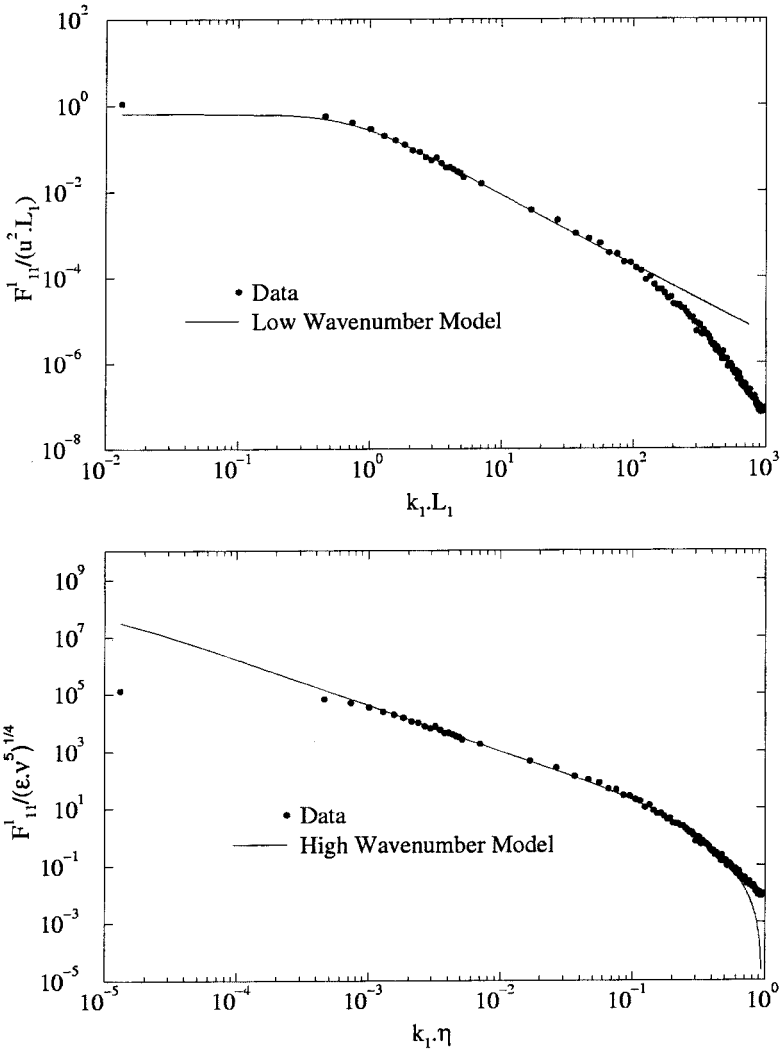

Figure 12. Low and high wavenumber models implemented separately at $R_\lambda = 473$.

the model to better simulate the spectral behavior at high wavenumbers. Finally Hill [13] extended slightly the model.

It is straightforward to modify the Lin/Hill spectrum to include the modified inertial subrange. The details are in [5]. The resulting functional form for the energy spectrum E at high wavenumbers is:

$$E^+_{\text{high}} = \alpha\,(1 + k^{+2/3})\,k^{+-5/3+\mu}\,\exp\left[-2\alpha\left(\frac{k^{+4/3+\mu}}{4/3+\mu} + \frac{k^{+2+\mu}}{2+\mu}\right)\right]. \qquad (76)$$

Note that the model reduces to the overlap power law form when $k^+ \to 0$ as required. Its substitution into the dissipation integral also yields the correct dissip-

ation, and this fact was used by us to determine the coefficients in a manner similar to that used by Lin and Hill.

Finally, using the isotropic relation between F_{11}^1 and E, we can implement the model for the one-dimensional spectrum. Figure 12 (lower) shows a comparison of the modified Lin/Hill one-dimensional spectrum and the Mydlarski/Warhaft data for $R_\lambda = 473$. The discrepancy at low wavenumbers is expected since the model is not valid there. The slight discrepancy at high wavenumbers is probably more due to the effect of measurement errors at these very low spectral values than to the model. Most importantly, the model captures the power law region and the high wavenumber departure from it accurately; and that is its primary reason for being introduced here.

A COMPOSITE MODEL

We now have two models for two different scaling regions, and a common overlap region (see Figure 12). We can therefore build a composite model to describe the spectrum in the *whole range of wavenumbers* by combining these two models. The simplest way to do this would be to simply add them, then subtract the common part. Unfortunately this possibility is precluded because the Lin/Hill spectrum is not integrable (nor our modification of it as well) because of the low wavenumber asymptote. (Note that only the energy is infinite, the dissipation is finite.) This problem can be resolved by using the other common approach to building a composite spectrum; namely, multiplying the two spectra together and dividing by the common part.

We define the composite model as the product of the low wavenumber and the high wavenumber models and divide by the common part. Note that there are two ways of expressing the common part, so

$$E_{\text{composite}} = \frac{(u^2\,L)\,\overline{E}_{\text{low}}(\overline{k}) * (\varepsilon\,\nu^5)^{1/4}\,E^+_{\text{high}}(k^+)}{(u^2\,L)\,C_L\,(\overline{k})^{-5/3+\mu}}, \tag{77}$$

or

$$E_{\text{composite}} = \frac{(u^2\,L)\,\overline{E}_{\text{low}}(\overline{k}) * (\varepsilon\,\nu^5)^{1/4}\,E^+_{\text{high}}(k^+)}{(\varepsilon\,\nu^5)^{1/4}\,C_H\,(k^+)^{-5/3+\mu}}.$$

It is easy to see from this why the multiplicative form leads to a useful result; the singularity in the high wavenumber of the modified Lin/Hill model when $k^+ \to 0$ is removed by the k^4 term from the low wavenumber form.

The model must satisfy three different constraint equations:

1. The kinetic energy:

$$\frac{3}{2}u^2 = \int_0^\infty E(k)\,\mathrm{d}k.$$

2. The integral scale:

$$L_1 = \frac{3\pi}{4} \frac{\int_0^\infty E(k)/k \, \mathrm{d}k}{\int_0^\infty E(k) \, \mathrm{d}k}.$$

3. The dissipation rate:

$$\varepsilon = 2\nu \int_0^\infty k^2 E(k) \, \mathrm{d}k.$$

Note that the constants determined for the high and low wavenumber models separately by using these constraint equations are not valid for the composite model. To determine the constants in the composite model, the three constraint equations must be applied to the composite model itself. These integrals, unfortunately do not have an analytical solution, so all integrations must be done numerically.

To fit the composite spectrum to each measured spectrum, only two parameters need to be specified: μ and either C_H or C_L (depending on whether the data were in high or low wavenumber variables). To begin, we used the values of μ found with Method 1; then we allowed the different constants in the model to vary to insure that the three constraint equations above were satisfied. This allowed the model to initialize the constants for the next search based on the value of μ found with the data. The final step was to let all the constants and μ change to optimize the fit with the data while still verifying the constraint equations. The resulting fits were shown earlier in Figures 7 and 8. For all spectra the agreement is more than satisfactory.

References

1. Barenblatt, G.I. and Chorin, A.J., New perspectives in turbulence: Scaling laws, asymptotics and intermittency. *SIAM Review* **40**(2) (1998) 265–291.
2. Batchelor, G.K., *The Theory of Homogeneous Turbulence*. Cambridge University Press, Cambridge, U.K. (1953).
3. Driscoll, R.J., The influence of spectral transfer and molecular diffusion on turbulent mixing and combustion. Ph.D. Thesis, SUNY at Buffalo (1982).
4. Frisch, U., *Turbulence*. Cambridge University Press, Cambridge, U.K. (1995).
5. Gamard, S., A new similarity analysis for the turbulence energy spectrum. Master's Thesis, SUNY at Buffalo (1999).
6. George, W.K., The self-preservation of turbulent flows and its relation to initial conditions and coherent structures. In: George and Arndt (eds), *Advances in Turbulence*. Hemisphere, New York (1989) pp. 39–73.
7. George, W.K., The decay of homogeneous isotropic turbulence. *Physics of Fluids A* **4**(7) (1992) 1492–1509.
8. George, W.K., Some new ideas for similarity of turbulent shear flows. In: Hanjalic and Pereira (eds), *Proceedings of Turbulence Heat and Mass Transfer Symposium*, Lisbon, Portugal. Begell House, New York (1994) pp. 24–49.

9. George, W.K. and Castillo, L., Zero-pressure-gradient turbulent boundary layer. *Applied Mechanics Review* **50** (1997) 689–729.
10. George, W.K., Castillo, L. and Wosnik, M., A theory for turbulent pipe and channel flows. *Theoretical and Applied Mechanics*. TAM872, UILU-ENG-97-6033 (1997).
11. Hanjalic, K. and Launder, B.E., Contribution towards a Reynolds-stress closure for low-Reynolds-number turbulence. *Journal of Fluid Mechanics* **74** (1976) 593–610.
12. Helland, K.N., Atta, C.W.V. and Stegen, G.R., Spectral energy transfer in high Reynolds number turbulence. *Journal of Fluid Mechanics* **79** (1977) 337–359.
13. Hill, R.J., Models of the scalar spectrum for turbulent advection. *Journal of Fluid Mechanics* **88** (1978) 541–562.
14. Kistler, A. and Vrebalovich, T., Grid turbulence at large Reynolds numbers. *Journal of Fluid Mechanics* **26** (1966) 37–47.
15. Kolmogorov, A.N., The local structure in incompressible viscous fluids for very large Reynolds numbers. *Comptes Rendus de l'Académie des Sciences U.R.S.S.* **30** (1941) 301.
16. Kolmogorov, A.N., A refinement of previous hypotheses concerning the local structure of turbulence in a viscous incompressible fluid at high Reynolds number. *Journal of Fluid Mechanics* **13** (1962) 82–85.
17. Launder, B.E., Second moment closure: Present . . . and future? *International Journal of Heat and Fluid Flow* **10** (1989) 282.
18. Launder, B.E., Reece, G.J. and Rodi, W., Progress in the development of a Reynolds-stress turbulence closure. *Journal of Fluid Mechanics* **68** (1975) 537–566.
19. Lin, J.T., Velocity spectrum of locally isotropic turbulence in the inertial and dissipation ranges. *Physics of Fluids* **15**(1) (1972) 205–207.
20. Monin, A.S. and Yaglom, A.M., *Statistical Fluid Mechanics*. Vol. II. MIT Press, Cambridge, MA (1975).
21. Mydlarski, L. and Warhaft, Z., On the onset of high-Reynolds-number grid-generated wind tunnel turbulence. *Journal of Fluid Mechanics* **320** (1996) 331–368.
22. Obukhov, A.M., On the distribution of energy in the spectrum of turbulent flow. *Comptes Rendus de l'Académie des Sciences U.R.S.S.* **32** (1941) 19.
23. Pau, Y.-H., Structure of turbulent velocity and scalar fields at large wavenumbers. *Physics of Fluids* **8**(6) (1965) 1063–1075.
24. Pau, Y.-H., Transfer of turbulent energy and scalar quantities at large wavenumbers. *Physics of Fluids* **11**(6) (1967) 1371–1372.
25. Sreenivasan, K.R., On the scaling of the turbulent energy dissipation rate. *Physics of Fluids* **27** (1984) 1048–1051.
26. Tennekes, H. and Lumley, J.L., *A First Course in Turbulence*. MIT Press, Cambridge, MA (1972).
27. von Karman, T. and Howarth, L., On the statistical theory of isotropic turbulence. *Proceedings of the Royal Society, London, Series A* **164** (1938) 192.